ANL/CP--73755

DE92 006977

High Level Seismic/Vibrational Tests at the HDR – An Overview

by

C. A. Kot, M. G. Srinivasan, B. J. Hsieh, Argonne National Laboratory;
D. Schrammel, L. Malcher, Kernforschungszentrum Karlsruhe, FRG;
H. Steinhilber, Fachhochschule Giessen – Friedberg, FRG;
J. F. Costello, U.S. Nuclear Regulatory Commission, Office of Research

ABSTRACT

As part of the Phase II testing at the HDR Test Facility in Kahl/Main, FRG two series of high–level seismic/vibrational experiments were performed. In the first of these (SHAG) a coast–down shaker, mounted on the reactor operating floor and capable of generating 1000 tonnes of force, was used to investigate full–scale structural response, soil–structure interaction (SSI), and piping/equipment response at load levels equivalent to those of a design basis earthquake. The HDR soil/structure system was tested to incipient failure exhibiting highly nonlinear response. In the load transmission from structure to piping/equipment significant response amplifications and shifts to higher frequencies occurred. The performance of various pipe support configurations was evaluated. This latter effort was continued in the second series of tests (SHAM), in which an in–plant piping system was investigated at simulated seismic loads (generated by two servo–hydraulic actuators each capable of generating 40 tonnes of force), that exceeded design levels manifold and resulted in considerable pipe plastification and failure of some supports (snubbers). The evaluation of six different support configurations demonstrated that proper system design (for a given spectrum) rather than number of supports or system stiffness is essential to limiting pipe stresses. Pipe strains at loads exceeding the design level eightfold were still tolerable, indicating that pipe failure even under extreme seismic loads is unlikely inspite of multiple support failures. Conservatively, an excess capacity (margin) of at least four was estimated for the piping system, and the pipe damping was found to be 4%. Comparisons of linear and nonlinear computational results with measurements showed that analytical predictions have wide scatter and do not necessarily yield conservative responses, underpredicting, in particular, peak support forces.

1. Introduction

The Heissdampfreaktor (HDR) Test Facility is located in Kahl/Main in the Federal Republic of Germany, 40 km east of Frankfurt/Main. It was built as a prototypical Superheated Steam Reactor in the period of 1965 to 1969 and shut down in 1971 after only 2000 hours of operation. After extensive decommissioning and conversion work it has been used since 1974 by the HDR Safety Project (PHDR) of the Kernforschungszentrum Karlsruhe (KfK) to perform vibrational/seismic, thermal hydraulic, blowdown, and other experiments related to the safety and design of nuclear power plants.

The overall objective of the HDR project is the experimental verification of calculational methods and procedures for use in reactor design and safety analysis, as well as the generation of experimental data and information that can be directly applied to power reactors. While the KfK, on behalf of German Federal Ministry of Research and Technology (BMFT), is responsible for the performance of the experiments, data acquisition, comparisons and evaluations, the efforts are, in general, carried out in collaboration with many industrial and government institutions both within

Germany and abroad. Specifically, the U.S. NRC Office of Research has collaborated with KfK in many of the research efforts at the HDR.

During the first phase of HDR testing in the time frame from 1975 to 1983, low and intermediate level vibrational experiments were performed on the HDR structures and equipment, using eccentric mass shakers, explosives, impact and snapback techniques [1]. In the second phase of HDR testing seismic margins tests of the reactor building, called SHAG, were carried out in 1986 using a large coast-down shaker located on the reactor operating floor. These were followed by failure and seismic margins tests of piping, called SHAM, which were performed in 1988. The U.S. NRC Office of Research through its contractors, Argonne National Laboratory (ANL) and Idaho National Engineering Laboratory (INEL), collaborated extensively in these latter two test series under a special agreement between KfK/BMFT and NRC for the HDR Phase II testing. In this paper interest is limited to the full-scale high-level seismic tests of the HDR building and piping, i.e., to the SHAG and SHAM tests. The following provides a brief description of the HDR Test Facility, the SHAG and SHAM tests, an overview of the results obtained from these experiments and related analyses, and discussions/conclusions emphasizing the implications for nuclear reactor safety and design.

2. HDR Test Facility

The HDR reactor building, Fig. 1, is a reinforced concrete and steel structure approximately 52 m high. It is embedded to a depth of 13 m giving the building an overall height of 65 m. The outer diameter is 22.4 m. The internal concrete structure consists of 2 concentrical cylinders interconnected by numerous walls and floors separating compartments for the mechanical equipment. The reactor pressure vessel is located at the center. It is 10 m in height, and has an inner diameter of 3.0 m and a wall thickness of 14.2 cm.

A steel containment with a wall thickness of approximately 3 cm encloses the inner structure, separated from it by a 2 cm thick styrofoam layer. The steel cylinder extends to a height of 40 m, where a polar crane is located (10 m above the operating floor) and is topped with the hemispherical steel dome. Personnel and equipment hatches are connected to the steel containment shell. The third part of the building, the external containment built out of reinforced concrete, is also a cylindrical shell with a hemispherical dome. The wall thickness is 60 cm and has little reinforcement because the HDR was not designed against external loads other than wind loads.

Finally, the basement consists of the foundation slab and a massive inner cylinder that forms an egg-cup like support for the inner structure. Structurally, this can be regarded as the only connection between inner steel containment and concrete containment. The two shells are independent of each other at all other points. The annulus between concrete and steel shells is 60 cm wide and is accessible. On one side of the reactor building is the crane and equipment tower and on the other side the operations building (Fig. 1). Because the site was previously used for brown coal mining activities, the soil characteristics were improved before construction by vibration injection of gravel columns down to the solid clay layers at 20 m depth. The ground water table is located 6 m below the surface.

An electrically heated boiler of 4 MW, permits the simulation of boiling water as well as pressurized water reactor conditions in the mechanical equipment and piping. Besides that, extensive facilities for measurement and data acquisition were installed, 400 fast (4 kHz) and 200 slow (2.5 Hz) measuring channels can be sampled simultaneously. This measurement/data acquisition system is connected through a data link with a data base at the PHDR/KfK in Karlsruhe. In addition to the experimental data, this data base also contains the results of calculations, which are performed for all experiments. This provides a sound basis for data evaluation and for the

verification of codes, mathematical modeling practices and assumptions (parameters and boundary conditions).

3. SHAG Experiments - Test Series T40

The centerpiece of the Phase II seismic/vibrational testing at the HDR was the high-level shaker test series (SHAG) which was performed in June and July of 1986 [1, 2, 3]. These tests in which the NRC/RES and many other organizations participated provided the culmination of the seismic testing of the reactor building that progressed through low and intermediate level testing in Phase I. The purpose was to investigate full-scale structural response, soil/structure interaction, and piping and equipment response under strong excitation conditions, i.e., under excitation levels that induce significant strains in the structure and soil and produce nonlinear effects in the soil/structure system and piping. As with all HDR experiments, the primary intent of the SHAG tests was to verify and validate calculational procedures and analysis methods. At the same time, the experimental data provide direct information on the response and performance of structural systems, piping, and equipment under high dynamic loading; such information may have direct applicability to understanding the behavior of nuclear power plant systems. Examples of this were the evaluation of various pipe support configurations in an in-plant piping system and the investigation of the performance of a typical U.S. gate valve under seismic loading.

3.1 Test Description

The excitation in the SHAG experiment was provided by a large eccentric-mass coastdown shaker designed by ANCO Engineers, Inc., capable of generating forces in excess of 1000 tons (metric) which was mounted on the operating floor of the HDR building as shown schematically in Fig. 2. The shaker was designed to develop maximum accelerations in the HDR building on the order of 5 m/s^2 and maximum displacements of about $\pm$ 7 cm. Test starting frequencies ranged from 1.6 to 8.0 Hz. Details of the shaker operation have been described previously [2, 3]. As the shaker revolutions (frequency) slow down and building resonances are traversed, the shaker energy is transferred to the building and the interior components. The increase in building response when the shaker reaches one of its resonances can clearly be seen in Fig. 3.

The primary purpose of the SHAG experiments was to subject the HDR Reactor Building, which was not designed for earthquake loads, to vibrational excitation up to incipient failure, where local damage could occur but global failure would be excluded. Other objectives included the study of load transmission through the structures and equipment, and the investigation of full-scale equipment and piping response. In particular the response of an in-plant piping system, called the Versuchskreislauf (VKL) with different multiple support configurations was evaluated.

A total of 460 channels of instrumentation was used during the SHAG tests to measure all important response parameters, including the safety aspects of the HDR and neighboring facilities [3]. In planning the SHAG tests, it was intended that the loading of the HDR facility not be limited by the excitation system but rather by the capacity of the building itself. Nearly all tests were designed to generate nominally the same peak force of 10^4 kN, at different starting frequencies of the shaker. Higher shaker frequencies (4.5 to 8.0 Hz) were intended primarily for piping excitation, while the lower frequencies (1.6, 2.1, and 3.1 Hz) were intended primarily to challenge the soil/structure system. A total of 25 experiments were performed, 10 of these were for the investigation of soil/structure system response, the remaining 15 served to study the VKL piping behavior. Of the latter, 5 tests were performed at pressurized water reactor conditions (210°C, 70 kN).

3.2 Reactor Building, Soil and Free Field - Result Overview

The HDR Reactor Building was essentially designed for dead weight and operational loads, with the only external load considered being the horizontal wind load. Hence, the building is very lightly reinforced particularly in the outer concrete containment (shield building). Prior to the tests extensive safety calculations were undertaken [4, 5]. These indicated that the reactor building could only be subjected to relatively low shaker eccentricities (about 10^4 kgm). Therefore, a procedure was established requiring that each test be accompanied by calculational safety evaluations and an immediate assessment of critical test measurements before proceeding with the next test.

During the preliminary shaker functionability tests it was established that the load distribution in the building is quite different from that assumed in the static safety calculations, and that a large share of the load (about 60%) is carried by the inner shell structure and the walls which are normally neglected in static calculations. Taking these aspects into account it was estimated that shaker tests with eccentricities of up to 10^5 kgm could be undertaken.

While the safety calculations predicted that the concrete foundation region would experience the highest stresses, it was found during the functionability tests, and confirmed by more refined calculations [5], that the greatest challenge to the building was in the outer concrete structure. Specifically, locations where floors are coupled to the outer structure (shell) and the embedded region of the outer shell were determined to be weak points. Therefore, these regions were extensively instrumented and samples were taken to determine the characteristics of the concrete. In the actual experiments masses of up to 25 tons per shaker arm were used, with the starting frequencies as planned between 8.0 and 1.3 Hz and eccentricities between 4,700 and 67,000 kgm. Peak forces of more than 10^4 kN (1000 tonnes) were reached as shown in Fig. 4.

3.2.1 Maximum Building Responses

As anticipated the highest stresses in the reactor building occurred in the outer containment (shield building) due to vertical membrane forces in the lower portion of the shell between the elevations of 0 and -11 m. This region is only minimally reinforced. The tensile forces which can be sustained by the reinforcement are less than those allowed for the concrete proper. Based on the measured cracking strength of the concrete the highest allowable membrane tensile stress was determined to be 0.5 MN/m^2. Obviously credit could also be taken for a compression stress of 1.1 MN/m^2 due to the dead weight of the concrete shell. The maximum allowable membrane stress was slightly exceeded in the tests.

There was extensive cracking of some interior floors, shifting and collapse of some masonry walls, and impact with neighboring structures. Nevertheless, the HDR-Reactor Building sustained no significant global damage. This, inspite of the fact that the building was not seismically designed and was subjected to peak accelerations of 0.4 g and displacements of ±5.0 cm, which correspond to an earthquake excitation of an intensity 7-8 on the Mercali scale. A comparison of the maximum building responses in the SHAG tests and a maximum credible earthquake in Central Europe is given in Fig. 5.

3.2.2 Reactor Building Frequencies and Damping

In earlier experiments [6] it had been clearly established that the reactor building response is dominated by rocking modes, nominally at about 1.5 Hz, and out-of-phase bending modes, at around 2.5 Hz, in which the outer concrete containment shell moves in the opposite direction to the inner steel shell containment. Both rocking and out-of-phase bending are associated with two very closely spaced modes, one in each of the horizontal directions (x and z).

A detailed system identification analysis indicates, that as the loads in the SHAG experiments were increased (from 4,700 to 8,200 kgm) the frequencies of the out-of-phase bending modes decreased by about 4% while the modal damping increased by about 30%. The latter consists primarily of structural damping in the concrete structures in the foundation region where the inner structure and the outer shell are coupled. The effect was even more dramatic for the two rocking modes, where as the load increased (from 4,700 to 67,000 kgm) the frequencies dropped by about 40% to around 1.0 Hz. At the same time the damping increased by about 50% to values as high as 9% of critical (see Fig. 6). This damping is composed of concrete structural damping, radiation damping, and hysteretic damping in the soil. However, the large frequency shifts are primarily caused by the reduction in shear stiffness which is associated with large shear deformations.

3.2.3 Load/Vibration Transmission

One of the objectives of the SHAG experiments was to investigate the transmission of vibrational energy from the shaker to the building, its large components and piping, the surrounding soil and adjacent structures. As shown in Fig. 3, the load transmission to various parts of the reactor building was primarily effected by energy transfer during the traversal of the various building resonances.

It is interesting to note that while the shaker excitation was limited to relatively low frequencies (8 Hz maximum), significantly higher frequency vibrations were measured at many locations throughout the building and particularly at mechanical components. Thus in the VKL piping, frequencies as high as 10-12 Hz were strongly excited. This is due primarily to nonlinear effects, such as impacts.

Response amplification was also in evidence at many locations and was particularly pronounced for the VKL piping. Here, velocities and accelerations were as much as 20 times higher than those in building proper. This is partially due to the fact that the VKL was not only attached to the building walls, but also to a large vessel (the HDU). The opportunity for double amplification of the motion, via nonlinear effects, was thus established. Other equipment which exhibited response amplification include the polar crane (factor of 3-4), the material lock (factor of 2), and the external crane structure (factor of 5-6) which was primarily excited during the traversal of the rocking mode. Because of its unique stiff mounting, only the reactor pressure vessel did not show any response amplification relative to the reactor building.

The operations building is adjacent to the reactor building and is connected to it by a bridge structure. During the SHAG tests this structure was coupled to the two buildings predominantly by friction and was displaced only by a few millimeters. The operations building proper, which has its dominant vibration mode at 3.1 Hz, experienced only very minor damage during the tests.

3.2.4 Foundation, Soil and Free Field Response

Using acceleration measurements and assuming rigid body behavior, it was determined that the foundation slab experienced only minimal torsional and vertical motions. The horizontal translational motions are essentially zero when bending resonance is traversed. On the other hand, there are significant rotational motions about the horizontal axes. Based on the relationship between the horizontal translations and the rotations, the center of rotation during the traversal of the rocking mode is determined to lie 15 m below the foundation slab.

Assuming no tensile stresses could be transmitted at the foundation–soil interface, nonlinear pretest calculations [7] indicated that considerable basemat liftoff would occur at the

highest possible shaker load. Based on the measurements in the experiment with maximum shaker eccentricity (67,000 kgm), there was no indication of liftoff. This was substantiated by post-test calculations [8] which show that properly reducing the soil stiffness and adjusting the damping to match the test results leads to considerable margin against basemat liftoff.

A pretest safety assessment of the possibility of soil liquefaction and building instability was performed by comparing the expected dynamic shear stresses with the normal stresses due to building and overburden loads. The estimates indicated that even for shaker loads in excess of those planned, there would be no danger of soil liquefaction. These conclusions were substantiated by pore pressure measurements during the SHAG tests, and extrapolation of the results confirm that the simple approach, used in safety regulations for estimating possible soil liquefaction, is valid [8].

A rotationally symmetric nonlinear finite difference model of the soil was coupled to a simple beam model of the HDR building [8] to predict the free field response in the SHAG experiments. It was found that even for shaker loads much larger than those planned, the free field vibrations at all neighboring installations would be very benign. During the tests actual loads were only about one half of those used in the safety assessments. The maximum measured vibration amplitudes in the free field occurred at higher frequencies during the rocking mode and were primarily horizontal responses. During the bending mode traversal, vertical responses were dominant.

3.2.5 Comparison of Calculated and Measured Soil-Structure Interaction Response

In addition to the safety assessments a number of predictive calculations were performed by German investigators for the soil-structure interaction response of the reactor building [9]. A best-estimate pretest safety prediction was also performed by Weidlinger Associates [10]. In the latter the site is represented by a fully 3-D finite element model with a nonlinear constitutive relation, and the containment building is represented by a beam model with the structure assumed as linear elastic. The structural beam model is coupled to the continuum site model at the soil-structure interface, and separation and recontact at the interface are included in the model. Lastly the shaker is modeled by the appropriate nonlinear rigid body dynamics equations which are coupled to the beam superstructure. The process of shaker arm closure, contact and energy transfer between shaker and structure are simulated.

Calculations using this model were performed with the FLEX Computer Code [10] to simulate the soil-structure interaction for two of the planned SHAG experiments with starting frequencies of 1.6 and 3.1 Hz respectively. The results of these computations were then used as input to a detailed finite-element analysis of the foundation and embedded region of the reactor building to determine the expected internal forces/moments and stresses. Since these calculations were performed for eccentricity values and/or shaker starting frequencies that were larger than those used in the actual tests, a direct comparison with measured values is not possible. However, qualitatively the predictions for both the soil-structure interaction and the detailed response in the embedded region are quite correct. Thus, no soil failure and no significant basemat liftoff were predicted. The maximum moments in the outer containment wall due to membrane tensions were also correctly shown to exceed the allowable moments.

The computational models used by German investigators included the following [8, 9]:

Model BHZ - Beam model with elastic coupling between between inner and outer structure; nonlinear soil-springs derived from a preliminary soil-structure interaction analysis.

Model CER - Beam model with elastic coupling between inner and outer structure; linear soil-springs.
Model IMB - Shell model of outer structure rigidly coupled to a beam model of the inner structure; linear soil-springs.
Model KUH - Beam model with elastic coupling of inner and outer structure; nonlinear soil-springs, decoupled in the two directions (CKUH) for pretest calculations and coupled (DKUH) in post-test calculations.
Model KWU - Rotationally symmetric shell model; linear soil springs.

In Fig. 7 the measured vibrational response (displacement) at the top of the outer containment is compared with the corresponding calculational results. Shown are the displacement amplitude envelopes as a function of shaker frequency which starts at 1.6 Hz and then decays. To understand the results it is essential to recall the test process. The excitation of the building starts during the closure of the shaker arms and the force increases until the arms are completely coupled at a frequency just above the building resonance frequency. As the displacement and soil deformation increase the soil stiffness and hence the resonance frequency decrease, i.e., the resonance frequency tends to decrease ahead of the excitation frequency. Since the excitation force decreases with the frequency, there is very little increase in the displacements until the actual traversal of the resonance frequency occurs (see Fig. 7).

The deviations of the calculational results from the experimental behavior seen in Fig. 7, can be directly related to the model characteristics and the selected parameters. It is thus possible to draw conclusions as to the advantages and disadvantages of the various approaches in representing the nonlinear building responses.

Qualitatively the nonlinear pretest calculations (BBHZ) and blind post-test calculations (CBHZ, CKUH) are similar to the test response. In particular they provide a good estimate of the actual resonance frequency. However, they overestimate the building response, because the damping used in all three cases was too low.

A linear simulation of the soil-structure response does not properly capture the actual behavior (see Fig. 7). Using a good estimate of the reduction in soil stiffness with increase in load as well as the appropriate damping, one can obtain good agreement with the experiment at the time of resonance traversal (Model CIMB). However, above the resonance frequency the building response is significantly underpredicted. If a soil stiffness is used that corresponds to a lower level of excitation and a lower damping value is selected (Model CKWU), the calculated resonance occurs at higher frequency and higher excitation forces, resulting in turn in higher response amplitudes than those measured. The erratic behavior around 1.5 Hz that is in evidence for two of the pretest calculations (BBHZ and BCER) can be traced to the fact that in these simulations the full peak shaker force is applied instantaneously, completely ignoring the transition phase during shaker arm closure. Based on the foregoing it can be stated that nonlinear modeling of soil-structure interaction is required in order to represent, at least qualitatively, the building response during the high level SHAG tests.

The SHAG tests also provided an opportunity to evaluate models and approaches used in probabilistic structural mechanics which take into account the uncertainties in structural and loading parameters by treating them as random variables [11]. In the current application the shaker loading was assumed to be given (deterministic), while the masses, stiffnesses, damping values, and concrete strength parameters of a structural model were treated as random variables. The parameters of the probability distributions were estimated on the basis of experimental data and values from the literature. The structural responses were determined by the Response Surface Method. Possible failure locations were postulated in the outer containment shell and foundation slab, and the exceedance of the concrete strength was used as the failure criterion. The failure probability was estimated using the Importance-Sampling Approach.

The analysis gave a failure probability of 2.2% for the foundation slab and 16.0% for the outer containment shell. Comparing these results with the usually accepted values of 10^{-6} for the probability of collapse or 10^{-3} for the loss of building functionality confirms that the HDR building was indeed tested up to incipient failure in the SHAG experiments, without inducing global damage.

3.3 Evaluation of the VKL Piping Responses In SHAG Tests

The VKL piping as used in the SHAG Experiments (Fig. 8), consists of a number of pipe runs ranging in nominal size from 100 to 250 mm. The piping is attached to the HDU vessel and associated manifolds and forms part of the experimental piping system at the HDR facility. The top of the pipe runs at about 28 m above ground level, just under the HDR operating floor (where the shaker is located). The original HDR hanger system provided primarily vertical dead weight support and consisted of six spring and constant-force hangers and one threaded rod. To avoid possible permanent damage to the VKL piping, two rigid struts, adjacent to the spherical tee (Fig. 8), were added to the support system. The intent in the SHAG tests was to compare the performance of this very flexible conventional support system (HDR system) with the behavior of hanger configurations designed for seismic loading and to evaluate their relative responses under indirect (through the building) loading at levels of excitation of a design basis earthquake.

The evaluation concentrated on five support configurations. These included the very flexible HDR system, the flexible KWU configuration with five struts (designed by KWU, Offenbach), the stiff NRC configuration with six struts and six snubbers (designed by INEL), the EPRI/EA configuration with three plastic dampers replacing the snubbers (designed by Bechtel Power Corp.), and the EPRI/SS configuration in which the six snubbers were replaced by seismic stops (designed by R. L. Cloud and Associates). Two additional configurations that used viscous dampers were tested each in a single experiment only. These were the GERB configuration and the ANCO configuration (designed by ANCO Engineers, Inc.). Support locations are indicated in Fig. 8 and the support arrangements used in each configuration are given in Fig. 9.

For each of the five evaluated configurations, three experiments were performed with nominally the same loading, i.e., the same shaker eccentricity and starting frequency. However, a direct comparison of the measured responses for the different configurations is not meaningful because of the dependence of shaker force on frequency. This results in higher loadings at higher frequencies. Hence, the more flexible (lower frequency) support configurations are less challenged in the tests. Therefore, the individual experiments were normalized by multiplying the measured responses by factors corresponding to the ratios of the maxima in the building response spectra (for each test) to the maximum value of a reference spectrum with a peak at 40 m/s^2 [3, 8].

The comparison of normalized peak responses (Fig. 10) does not indicate any advantages for a stiff support system (NRC) relative to a reasonably designed flexible (KWU) system. However, the very flexible HDR configuration, which was not designed seismically, results in unacceptably high displacements and stresses. The snubber replacement configurations, i.e., energy absorbers and seismic stops, proved themselves in that they performed as well as the NRC configuration. However, the seismic stops resulted in some local high level impact loads [3, 8].

A number of comparison calculations for the VKL response in the SHAG tests were undertaken by German and U.S. investigators [8, 12]. In general, the computational predictions showed considerable deviations from the experimental results. These discrepancies can be partially attributed to modeling; i.e., differences in masses, stiffnesses, and representation of supports; and partially to the idealization of the excitation in the calculational models. However,

the dominant factor for the lack of agreement between measured and calculated results can be attributed to the poor definition of boundary conditions of the VKL piping in the SHAG tests. In the experiments the VKL piping was not properly isolated or disconnected from other piping and the stiffnesses of anchors were not defined. These effects strongly contributed to the response of the VKL piping, but could not be represented in the computational modeling.

4. SHAM Experiments - Test Series T41

As the last series of tests in Phase II of the HDR Safety Program, high-level seismic experiments, designated SHAM, were performed on an in-plant piping system during April and May 1988. The objectives of the SHAM experiments were to (i) study the response of piping subjected to seismic excitation levels that exceed design levels manifold and which may result in failure/plastification of pipe supports and pipe elements; (ii) provide data for the validation of linear and nonlinear pipe response analyses; (iii) compare and evaluate, under identical loading conditions, the performance of various dynamic support systems, ranging from very flexible to very stiff support configurations; (iv) establish seismic margins for piping, dynamic pipe supports, and pipe anchorages; and (v) investigate the response, operability, and fragility of dynamic supports and of a typical U.S. gate valve under extreme levels of seismic excitation.

The SHAM experiments were conducted as a cooperative effort among a number of organizations in Europe and the USA. These included KfK/PHDR, with the participation of the Fraunhofer Institut für Betriebsfestigkeit (LBF), Darmstadt, FRG, and the Kraftwerk Union (KWU), Offenbach, FRG; the Central Electricity Generating Board (CEGB), UK; the Electric Power Research Institute (EPRI), Palo Alto, California, with the participation of Bechtel Power Corp. and R. L. Cloud & Associates; and the U.S. Nuclear Regulatory Commission, Office of Research (NRC/RES), which supported the efforts of Argonne National Laboratory (ANL) and Idaho National Engineering Laboratory (INEL).

4.1 Description of the SHAM Experiments

The test object in the SHAM experiments was again the VKL piping system that was already extensively tested in the SHAG experiments. In the latter tests, excitation of the piping resulted from the shaking of the HDR containment building. In the SHAM experiments, direct, high-level shaking of the VKL piping was used. Therefore, some significant modification of the test loop was necessary. An isometric sketch of the VKL piping as used in the SHAM testing is shown in Fig. 11. The VKL consists of multiple stainless steel pipe branches ranging from 100 to 300 mm in diameter, with the main two flow loops connected to the HDU vessel and the DF16 manifold. A third major branch connects the DF16 manifold to the DF15 manifold. Aside from the pipe hangers and dynamic supports, the only points of fixity for the entire system, including the HDU and manifolds, are the supports at the bottom of the HDU and the nearly rigid attachment of the DF15 manifold. All extraneous piping leading to other flow systems in the HDR were disconnected for the SHAM tests. As in the earlier tests, the test loop again included an 8" U.S. gate valve from the decommissioned Shippingport Atomic Power Station. (For details see Ref. 13, 14, and 15.)

The VKL piping was excited directly by means of two servohydraulic actuators rated at 40 tonnes (metric) of force each. As shown in Fig. 11, both actuators were acting in the horizontal x-direction at hanger location H5 and at location H25 (DF16 manifold). The excitation system was designed and furnished by LBF-Darmstadt, FRG, and included a computer-controlled hydraulic actuating/control system to provide predetermined displacement-time histories. Extensive pretest design calculations indicated that the hydraulic shakers would be capable of producing up to 6 g acceleration for the VKL piping, with a maximum displacement (stroke) of ± 125 mm [14].

Six different dynamic support systems were designed for the VKL piping by the various participants in the SHAM testing. These ranged from the very stiff NRC system with rigid struts and snubbers, designed by INEL, to a very flexible HDR system with essentially only dead–weight supports. The supports of the NRC system were designed as weak as possible to permit the investigation of support failures. Two support configurations, provided by EPRI in collaboration with industrial partners, contained snubber replacement devices. The first of these, designed by Bechtel Power Corp., uses Energy Absorber (EA) devices, in which a set of specially designed steel plates is plastically deformed to dissipate energy and restrict pipe motion under seismic loading. The second snubber replacement system, designed by R. L. Cloud & Associates, Inc., includes Seismic Stops (SS). In their current design, these stops are simple telescoping–tube devices with preset internal gaps that allow a certain amount of motion to accommodate thermal effects. During seismic excitation, the motion is restricted/stopped by impacting on disc spring pads. Two other support configurations, designed by KWU and CEGB, rely only on rigid struts for dynamic restraint and attempt to optimize the number of supports. Figure 12 shows an overview of all the support configurations with the location and type of dynamic support clearly indicated. All configurations used the same dead–weight hanger system shown in Fig. 11. Similarly, all configurations employed the same rigid struts at locations H4 and H23. These are horizontal struts in the z-direction and their primary function is to stabilize the input motions of the actuators, at H5 and H25 respectively, so that they move only in the x-direction. The components of these supports were sized for the highest loads anticipated.

All dynamic support systems, except the CEGB configuration, were designed for the common HDR spectrum shown in Fig. 13. The actuators were displacement controlled, and the basic earthquake displacement history used was an artificially generated displacement–time function of 15 seconds duration fitted to the preselected common Safe Shutdown Earthquake (SSE)–floor–response spectrum with a 0.6 g peak acceleration (ZPA), shown in Fig. 13. The CEGB hanger system was designed for the Sizewell B spectrum (Fig. 13) which peaks at lower frequency than the common HDR spectrum.

Nearly 300 channels of data were recorded, with major measurements being strains, accelerations, displacements, and forces. Details of the instrumentation and data acquisition have been reported elsewhere [13, 14, and 15].

Fifty–one individual experiments were performed with the VKL piping and the six different pipe support configurations (see Fig. 14). Two random excitation tests of 120–s duration, with each of the hydraulic actuators singly and separately (H5 and H25) were performed for each hanger configuration. These tests provided dynamic characterization of the systems in the frequency range from 2 to 40 Hz.

For all but the CEGB configuration, earthquake experiments were then performed at the low to intermediate level, i.e., at excitation levels ranging from one SSE (0.6 g ZPA) to three/four SSE. These experiments were carried out with the 15–s duration displacement history based on the common HDR spectrum scaled to the proper SSE level. The two hydraulic actuators (at H5 and H25) were operated together and in phase; both were programmed to provide identical displacement histories. The purpose of these tests was to study the behavior of piping systems at load levels exceeding the design load and to compare the performance of different support configurations. These tests were also intended to provide seismic–margin information for dynamic supports, and data for the validation of linear analyses.

Two configurations, namely the KWU system and a modified NRC system [16], were then tested to high levels of excitation (up to 800% SSE) again with scaled–up displacement histories and both actuators operating in phase. The purpose of the high–level tests was to obtain information on possible pipe failure/plastification, seismic margins for piping, and pipe supports, and to provide data for the validation of nonlinear analysis methods.

The CEGB configuration was subjected to its own test program. Low– and intermediate–level earthquake tests were performed with displacement histories of 20-s duration derived from Sizewell B spectrum and an Allsites spectrum [Fig. 13]. Intermediate– and high–level tests were also performed with sine burst histories near the piping resonance, with a duration of 7.0 s and maximum displacement of 60 mm. Finally, to provide a comparison with the other configurations, a 100% SSE earthquake test was performed with the displacement history derived from the common HDR spectrum.

4.2 Highlights of SHAM Experimental Results

Detailed result overviews and discussions have been provided in earlier publications [13, 16]. Following the system identification tests with random excitation, simulated earthquake experiments were performed with all support configurations. The overall sequence of events during these tests and the approach are best illustrated on the basis of the strain measurements at cross-section 7 close to the "Tee" shown in Fig. 15. In this figure the range of strains between the upper and lower limits for each test is given by the bold vertical bar. The thinner horizontal connecting lines between those bars give the permanent strains remaining after each test. The sequence of bars from left to right corresponds to the test sequence.

In the first series of experiments with the HDR-spectrum the excitations were limited to such levels so as not to exceed the nominal support forces by more than a factor of four and to limit the strains in straight pipe sections to 0.2% and in elbows to 0.4%. For all the configurations designed for this spectrum, loads up to 300% SSE could be sustained without significant problems except for the malfunctioning of two snubbers. These were replaced by snubbers of different design but similar capacity.

Comparison tests were then performed with the 100% SSE HDR spectrum loading for the HDR and CEGB configurations. The latter was then tested at 100% and 300% of its design spectrum (Sizewell B) and at 50% and 200% loading corresponding to the Allsites Spectrum. The second series of tests was concluded with a 200% SSE (HDR Spectrum) test of the HDR support configuration.

The modified NRC configuration [13] was then subjected to loads up to eight times of the design earthquake. At 600% SSE three snubbers failed due to overload, these were not replaced. At 800% SSE an additional snubber failed without damage to the piping or excessive pipe deformation. These tests also caused the failure and/or loosening of some typical support anchors.

The purpose of the following sine-burst experiments with the CEGB configuration was to induce the so called "ratcheting" phenomenon, through the combined action of the static loads (internal pressure and dead weight) and the dynamic vibration excitation. This effect can be clearly seen in Fig. 15, where the permanent strains grow monotonically from test to test, on the top side of the pipe as tensile strains and on the bottom side as compressive strains. The resulting global deformation of the piping remained quite limited. Therefore, it was possible to perform the tests with the KWU configuration at 400%, 600% and 800% SSE loading (HDR-spectrum) without repairing the piping. Again in these tests the piping did not fail.

4.2.1 Piping Stresses/Strains

An impression of stresses/strain levels in the SHAM experiments can be obtained from Figures 16 and 17. The fictitious elastic bending stresses at cross-section 7 (see Fig. 15) in the small diameter pipe reached 600 MPa (Fig. 16), far into the plastic regime, with the permanent

strains exceeding 1%. Similarly, the amplitudes of the local strains at Elbow 1 (see Fig. 15)also reached about 1% (Fig. 17).

Comparisons of the response of the VKL piping with the various support configurations, at design level loading (100% SSE), were extensively discussed in References 13 and 16. Of primary interest are the stresses in the piping. Examining the maximum values of the bending stresses which are dominant under dynamic loading, it was found (see Figures 10 and 11 of Reference 13), that at most locations the stiff NRC-configuration had the lowest stresses. However, the differences relative to the KWU-configuration and the two EPRI configurations was insignificant. The pipe region in the vicinity of the excitation point at the DF16 manifold exhibited relatively high stresses for all configurations. In the remainder of the 200 mm piping the peak stress values were all quite low (10-40 MPa).

None of the configurations designed for the HDR spectrum demonstrated any particular advantage or disadvantage relative to stress levels. On the other hand the HDR configuration, which was not seismically designed, and the CEGB configuration, which was designed for another spectrum, exhibited much higher stresses in the 100/125 mm piping.

A direct link between the number of dynamic supports and the piping stresses could not be established. A similar conclusion was already reached in the SHAG tests in which the piping was subjected to indirect excitation through the building. Hence, it can be reiterated that of primary importance to the stress levels in the piping is the proper design of the support system for the actual loading spectrum, and not the number and type of supports or the overall stiffness of the support configuration.

The stress allowables used in the design process for earthquake loading are based on nominal (minimum) material strength parameters. Actual material strengths are usually significantly higher than those values. This approach is used to prevent the plastification of substantial regions of the piping and thus to avoid pipe collapse or ratcheting. For the very tough steels used currently in reactor construction these stress allowables are set much lower than is necessary in order to avoid crack formation during seismic excitation.

This is clearly illustrated in Fig. 18 which gives the allowable strain for the austenitic steel (DIN 1.4961 - German Norms) for Level D conditions as well as fatigue cycle curve for the material based on the German Standard KTA 3201.2. It can be seen that the material can sustain up to 10^4 cycles at the allowable strain level. A comparison of the actual strain amplitude frequencies experienced in the SHAM tests at two highly stressed locations and the fatigue cycle curve can also be made on hand of Fig. 18. The differences between these curves indicate that the entire SHAM test series would have to be repeated approximately 40 times in order to reach the fatigue life of the material. This provides clear evidence that a single earthquake event has no influence on the fatigue life of piping components. For the very few high level vibration cycles experienced in a typical earthquake excitation, the stress allowables used in the design procedures are thus very conservative.

4.2.2 Support Loads and Response

The dynamic supports used in the SHAM experiments included struts, snubbers, energy absorbers and seismic stops. The other supports, such as spring and constant force hangers, carry primarily the static loads and do not influence the dynamic behavior. In the tests each of the support types was separately investigated in at least one support configuration.

Intuitively, one would expect support loads to decrease with an increase in their number. However, it is actually possible to increase the loads by the introduction of additional supports, i.e., there is no direct correlation between the number of supports and the magnitude of the

loads. The design of a particular configuration is much more important than the number and type of supports. Similarly the failure of supports during the tests did not necessarily lead to increased loads at other supports or increased stresses in the piping. In particular, the failure of snubbers under overload occurred as individual events without having a direct effect on neighboring supports (no "Zipper Effect").

The snubber replacement devices again performed very satisfactorily. The impact forces in the current seismic stops with disc-spring impact pads were significantly reduced and were hardly greater than those occurring during snubber lock-up.

Twelve different struts were used in the experiments (2 manufactures, 3 sizes). None of them failed in spite of the fact that some of them repeatedly were subjected to loads exceeding the expected fourfold margins. A total of 15 snubbers were used. In contrast to the struts, 4 out of 9 snubbers, that experienced overloads, failed outright. In addition, at least two additional snubbers malfunctioned in that they allowed excessive travel and had a reduced load bearing capacity. Not all snubbers were able to sustain the expected threefold margin (relative to their nominal capacity). All snubbers failed under overload without any external signs of damage. In all cases the failed snubbers lost their capacity to transmit loads and their motion was unrestricted until internal impact occurred (behavior similar to seismic stops).

4.3 Damping

Damping values currently used in the design of nuclear piping are chosen very conservatively. They take account of external damping effects by allowing larger damping values for larger diameter pipes. The effect of load level on internal damping is accounted for by using higher damping values for the SSE than for the OBE. Because in most vibrational investigations of piping, the damping values have been found to be higher than those typically specified in design codes (1-2%), damping has been a subject of much debate. Recently it has been proposed both in the USA [17, 18] as well as in Germany [19] that more realistic damping values be introduced into the design process for nuclear piping systems.

The motivation for this is that conservative damping values lead to stiff piping system designs under seismic loading, and this, in turn, leads to significant disadvantages in accommodating normal operational loads. Also, there exists a considerable amount of earthquake experience indicating that flexible piping systems do not fail under seismic loading. Lastly the evidence of the SHAM experiments show that the flexible KWU configuration performed as well as the very stiff NRC system under extreme seismic loading without sustaining any damage.

Because of this background it was important that the damping in the SHAM experiments be evaluated very carefully, in particular, since the SHAM tests offered many advantages over other piping vibrational tests. These are: (i) a fairly prototypical piping system (branches, nozzle connections to vessels, different pipe diameters), (ii) the excitation was earthquake-like, (iii) the loads/stresses were increased stepwise far beyond the yield point, and (iv) the same piping system was investigated with different support configurations. Hence, the procedures used in the damping evaluation were also much more sophisticated than the typical single-degree-of-freedom approaches. Parameter identification techniques were directly applied to the measured data of the random tests with curve fitting over all modal frequencies and measurement locations done simultaneously. For the seismic experiments parameter variation calculations were used to fit the individual modal damping values at different loading levels.

Figure 19 presents the damping values as a function of frequency for three support configurations (HDR, KWU, NRC) as derived by parameter identification from the random test data. On the average these results show a tendency for the damping to increase with the number of dynamic supports. However, the difference in the mean damping value between the flexible

KWU system (3.92%) and the stiff NRC configuration (4.15%) is fairly minimal. Note that there are individual modes with either very weak (0.9%) or very strong damping (9.5%).

The dependence of damping on the loading magnitude, as obtained by parameter-variation calculations for individual modes in the earthquake experiments with the KWU configuration, is presented in Fig. 20. These results are compared with damping values used in existing regulatory codes or proposed in new standards. For most of the presented modes there is an increase in damping as the loads increase from 300% to 400% SSE. However, inspite of a modal stress of 500 MPa the damping does not increase for Mode 2. No correlation seems to exist between the calculated modal stresses and the damping values. On the other hand there is a correlation between the system damping (average of six relevant modes) and load level, namely damping decreases as the load increases from 100% to 200% (3.2 to 3%), then remains constant as the load increases from 200% to 300%, and then increases more rapidly (to 3.7%) as the load increases to 400%.

Qualitatively this behavior is in agreement with earlier experience and is due to the fact that there are damping mechanisms for which the damping force is independent of the vibration amplitude (e.g., friction forces). These decrease proportionally with increasing amplitude, while other damping mechanisms (e.g., material damping) come only into play at higher amplitudes. However, it is surprising that the latter effect only became effective in the earthquake tests at loading levels at which stress allowables for Level D were exceeded at a number of locations and the yield point was exceeded at many other points in the piping system.

Comparing the derived damping values with the standards, it is seen that existing codes such as the German KTA Standard are very conservative. On the other hand, the proposed PVRC damping of 5% [17] and the damping values of 7.5% proposed by Hadjan [18], are too high. The latter values were obtained by extrapolation from fairly low level experiments (stresses usually less than one half of yield [18]), and do not appear to be substantiated by the SHAM test results in which the yield limit for the piping materials was substantially exceeded.

The newly proposed German KTA standard [19] with a uniform damping of 4% appears to be quite realistic on the basis of the SHAM test results. For a given seismic spectrum the application of this damping value will not necessarily always yield conservative values for specific pipe stresses. However, there are sufficient additional conservatisms embedded both in the definition of the design spectrum and even more so in the stress allowables (as again evidenced by the SHAM results) to assure that safe designs will result.

4.4 Comparison of Computational and Experimental Results

The different pipe support configurations in the SHAM tests were all designed for a given loading spectrum using typical design analysis procedures. A detailed comparison of calculational results with the measured data indicates [13, 20] that typical design analysis procedures (time-history analysis, response spectrum methods) are not necessarily conservative, even when superposition of the responses in different excitation directions (3D–Excitation) was used. Real conservatisms are only introduced through spectrum broadening or the selection of proper damping values. Most importantly it was found that the design analysis, at least in this application, underpredicted the maximum dynamic support forces.

The purpose of most of the post-test calculations was to verify how well the piping response could be represented by linear modeling using realistic damping values and the actual excitation loads. In order to provide a certain variability in modeling and calculational approaches, three different German institutions were involved in the post-test analyses. In all their modeling Rayleigh damping is used as was also the case for the KWU pretest calculations [20]. Figure 22 gives a statistical evaluation obtained by comparing the maximum values of the four linear German

predictions, including the KWU pretest analysis (BKWU), with the corresponding measured values (KWU configuration, 100% SSE test). The mean values, standard deviations, and smallest/largest values for acceleration, strut forces and bending stresses are given. Values larger than 1 indicate calculational overestimates and values smaller than 1 are underestimates. In the statistical evaluation the results at all measurement locations were equally weighted, regardless of the absolute value.

In general, the accelerations and support forces are underpredicted and the mean values of the calculational results differ little from each other, with the exception of model CKWU for the accelerations and CMPA for the strut forces. The mean values for the stresses are all close to unity, i.e., in the mean the calculations essentially provide a good estimate of the maximum stresses.

Similar linear computations were performed by ANL [21] for both the KWU and NRC configuration. As seen in Fig. 22, the statistical evaluation of the results is not very different from that of the German studies. Again support forces and accelerations are underpredicted and the variability in the results is quite large. The best estimate is obtained for the pipe stresses. The large discrepancies relative to the measurements, for the accelerations and support forces, are related to higher frequency components in the measurements that result from the nonlinearities in the actual system. It is gratifying to note that pipe stresses, which govern the design, are at least in the mean, relatively well estimated by the calculations.

To account for the inherent nonlinearities of some of the supports (energy absorbers, seismic stops, snubbers), nonlinear modeling was used to estimate their response [20]. In the mean the results are somewhat closer to the measurements than those of the linear models, in particular, for the forces in the nonlinear supports. However, the insignificant improvement in predicting the forces in the remaining supports, the accelerations and the stresses, does not justify the large calculational effort required for the nonlinear time-history analyses.

Extensive nonlinear material response in the 800% SSE test with the KWU configuration was limited to the two most highly stressed pipe regions. This made it possible to estimate the local nonlinear effects using a simplified approach in which the nonlinear contributions to global behavior of the affected regions are derived from static calculations and added to the linear response [20, 22]. Extending the method to time history analysis and using parameter variation computations, it was possible, with this approach and reasonable computational effort, to define the essential differences between linear and nonlinear structural responses.

Fully nonlinear simulations of the 800% SSE test with the KWU support configuration were carried out by ANL using the NONPIPE computer code [23]. The elastic-plastic behavior in this case is modeled by assuming moment-curvature and torque-twist relationships to be trilinear and by an approximate treatment of strain hardening based on this trilinearity. There is again significant variability in the quality of the predictions. The results are statistically evaluated by comparing maximum values of the prediction to measurements for accelerations, strains, and support forces. As seen in Fig. 23, the mean values of the nonlinear predictions are, in general, better than those for the low level tests using linear analysis. While support forces are still underpredicted, the results are closer to the measurement. The best predictions are obtained for the strains. Some of the outliers in the latter are due to the fact that the calculations predict strain ratcheting at some locations. This phenomenon did not occur in the test because the material had been strain-hardened in preceding experiments.

4.5 Seismic Margins Evaluation

Because of their reasonable prototypicality in support design, piping layout and seismic excitation, the SHAM experiments provided an opportunity to demonstrate that piping systems

designed to current practice have large margins against failure and to quantify the excess capacity of pipe components and dynamic supports. Such an evaluation was undertaken [24] using both the system design information and the experimental measurements for the KWU and NRC configurations.

Different design approaches, standards and philosophies were used in the two system designs, resulting in some discrepancies in support strength and allowable stress values. To account for this, the design results were normalized to a common basis (Level C allowables) and margins were adjusted by overdesign factors [24]. Seismic margins were estimated for both the piping itself and the dynamic supports. These were calculated in two ways. On one hand design load level was used as a basis and on the other hand component capacity was used. Both of these estimates give deterministic excess capacities and do not represent seismic margins in the probabilistic sense.

Based on loading level alone, it was determined that the margin against pipe failure is at least 8 (KWU configuration). However, using the yield strain as an indication of nominal capacity, it was found that the excess capacity for the pipe material is at least 4. Similarly, for the struts, the margin against failure based on load level alone appears to be at least 8, since no struts failed even at 800% SEE. For the snubbers, the same margin is about 3 because some malfunctions occurred at that level. Taking into account overdesign and comparing the actual forces experienced by a particular support with its capacity, the lowest margin for snubbers is found to be about 2, and for struts, on the order of 6. Finally, making allowances again for overdesign, the SHAM tests show that the margin for the overall piping system is at least 4. This clearly demonstrates again the ruggedness of piping systems when subjected to the seismic loading.

5. Discussions and Conclusions

The high level vibrational/seismic experiments at the HDR have provided much useful information and insight concerning the behavior of reactor systems, piping, and components. Thus, in the SHAG experiments the reactor building was tested to incipient failure, as indicated both by measurement and probabilistic structural analysis, demonstrating that even structures not designed for earthquake loading have considerable capacity to resist such loads. The data show that as loads are transmitted from the building to equipment/piping considerable response amplification (up to 20 times in the SHAG tests) may be expected. Also nonlinear effects, such as impacts, may shift the response spectra to significantly higher frequencies than those contained in the excitation proper. The soil–structure interaction phenomena at the SHAG load levels (approximately equivalent to SSE loads) were inherently nonlinear as indicated by strong rocking mode frequency reduction and simultaneous increases in damping. Hence, in any computational modeling of soil–structure interaction response it is essential to include the nonlinear effects, such as the reduction in soil stiffness and shear modules with increasing deformations.

The SHAG experiments also demonstrated that piping systems with well designed compliant dynamic support configurations perform as well as those with stiff support configurations. It was also found that snubber replacement devices (energy absorbers and seismic stops) perform as well as snubbers in limiting pipe stresses. These findings were further amplified in the SHAM test series where six different support configurations were subjected to seismic loads exceeding design levels manyfold. In the latter tests it was also found that there is no correlation between the number of supports and pipe stresses as long as the support system is properly designed for the given seismic input spectrum.

The SHAM test again established that piping is very rugged in resisting seismic loads and that inspite of significant local pipe plastification and multiple support failures, there is no danger of pipe failure during the limited number of high loading cycles occurring in a typical earthquake. Similarly rigid struts were found to be very strong; none of them failed in the tests inspite of the

fact that some of them experienced six–fold overloads relative to their nominal capacities. Failures and malfunctions did occur in snubbers, some at loads less than three times their capacities. However, the failures of individual supports did not necessarily result in load increases at other supports and/or pipe stress increases. The overall margin or excess capacity for the piping system was found to be at least four.

A detailed and careful evaluation of pipe damping up to load levels of 400% SSE resulted in an overall system damping of approximately 4%. This indicates that piping damping values used in current codes and standards are conservative. On the other hand some of the proposed pipe damping values that are based on extrapolation from lower level tests appear to be too high.

Finally, extensive comparisons between measurements and both linear and nonlinear calculations showed that considerable scatter can be expected in the prediction of pipe response. Further calculational procedures, whether they be design or best estimate calculations, are not necessarily conservative in predicting peak responses. In particular, peak support forces may be significantly underpredicted. In general, the best predictions are for pipe stresses which govern the piping design and the inherent conservatisms built into the design process assure that piping systems are ruggedly designed and in no danger of failing under seismic loads.

References

1. L. Malcher and H. Steinhilber, "A Review of 15 Years Full–Scale Seismic Testing at the HDR," Trans. 11th Intl. Conf. on Structural Mechanics in Reactor Technology, Vol. K1, paper No. K15/1, pp. 397–408, Tokyo, Japan, 18–23 Aug. 1991.

2. L. Malcher and C. A. Kot, "HDR Phase II Vibrational Experiments," Proc. U.S. NRC 14th Water Reactor Safety Information Meeting (27–31 Oct. 1986), NUREG/CP–0082, Vol. 3, pp. 295–312, Febr. 1987.

3. C. A. Kot, L. Malcher and H. Steinhilber, "Vibrational Experiments at the HDR: SHAG Results and Planning for SHAM," Proc. U.S. NRC 15th Water Reactor Safety Information Meeting (26–29 Oct. 1987), NUREG/CP–0091, Vol. 3, pp. 251–277, Febr. 1988.

4. F. Stangenberg and R. Zinn, "Structural Safety of HDR Reactor Building During Large Scale Vibration Tests," Trans. 8th Intl. Conf. on Structural Mechanics in Reactor Technology, Vol. K(b), paper No. K20/11, pp. 473–478, Brussels, Belgium, 19–23 Aug. 1985.

5. H. Werkle and G. Waas, "Computed Versus Measured Response of HDR Reactor Building in Large Scale Shaking Tests," Trans. 9th Intl. Conf. on Structural Mechanics in Reactor Technology, Vol. K1, paper No. K9/3, pp. 479–487, Lausanne, Switzerland, 17–21 Aug. 1987.

6. P. Jehlicka, L. Malcher, H. Steinhilber and B. Brendel, "Earthquake Investigations at the HDR–Shaker Experiments at Intermediate and High Excitation Level" (In German), Quicklook Report V63, Technical Report PHDR 13–80, July 1980.

7. B. Weber and J. P. Wolf, "Earthquake Investigations of the Reactor Building, Nonlinear Soil–Structure Interaction," (In German), Elektrowatt Ingenieurunternehmung AG, Zürich, Working Report PHDR No. 4.290/85, Aug. 1985.

8. L. Malcher and H. Steinhilber (editors), "Structural Dynamics Investigations at the HDR, Earthquake Experiments up to the Load Bearing Capacity of the Reactor Building," (In German), Evaluation Report: SHAG, Technical Report PHDR 90–89, March 1990.

9. H. Steinhilber, G. Flade and D. Schrammel, "Approach and Status of the Evaluation of the Earthquake Experiments with the Large Building Shaker," (In German), 11th Status Report of the HDR Safety Program, Contribution No. 10, PHDR Working Report 05.37/89, 9 Dec. 1987.

10. D. K. Vaughan, R. Mak, and T. Piland, "Analysis of the HDR Containment Structure Subjected to High Level Shaker Loading," Weidlinger Associates, Final Report for ANL Contract No. 5152401, R 8663 DV, March 1987.

11. G. I. Schueller, H. J. Pradlwarter and P. Jehlicka, "Failure Probability of the HDR–Containment under Shaker Loading," Trans. 10th Intl. Conf. on Structural Mechanics in Reactor Technology, Vol. M, paper M06/2, pp. 149–154, Anaheim, CA, 14–18 Aug. 1989.

12. B. J. Hsieh, C. A. Kot and M. G. Srinivasan, "Vibration Testing and Analysis of a Multiply Supported Piping System," Trans. 9th Intl. Conf. on Structural Mechanics in Reactor Technology, Vol. K2, pp. 969–974, Lausanne, Switzerland, 17–21 Aug. 1987.

13. C. A. Kot, M. G. Srinivasan, B. J. Hsieh, L. Malcher, D. Schrammel, H. Steinhilber and J. F. Costello, "SHAM: High–Level Seismic Tests of Piping at the HDR," Nuclear Engineering and Design, Vol. 118, pp. 305–318, 1990.

14. L. Malcher, H. Steinhilber and D. Schrammel, "Design Report–HDR Test Group SHAM T41," (In German), PHDR Working Report 4.338/88, March 1988.

15. H. Wenzel, L. Löhr and R. Grimm, "Test Protocol – HDR Test Group SHAM T41, Volume I: Overall Test Sequence," (In German), PHDR–Working Report 4.345/88, 20 April to 27 May, 1988.

16. H. Steinhilber, L. Malcher and D. Schrammel, "Seismic Margins Tests of a Piping System at the HDR Facility," Trans. 10th Intl. Conf. on Structural Mechanics in Reactor Technology, Vol. K2, pp. 757–762, Anaheim, CA, 14–18 Aug. 1989.

17. Pressure Vessel Research Committee (PVRC), "Damping Values–Piping Systems, Technical Position and Justification," 1987.

18. A. H. Hadjian and H. T. Tang, "Piping System Damping Evaluations," Proc. Second Symposium on Current Issues Related to Nuclear Power Plant Structures, Equipment and Piping, EPRI NP–6437–D, Session 10, pp. 43–65, May 1989.

19. KTA 2201.4 (Proposed new German Standard), "Design of Nuclear Power Plants Against Seismic Influences, Part 4: Requirements for Procedures for the Verification of Earthquake Safety of Mechanical and Electrotechnical Components," Version 6/89.

20. D. Schrammel and H. Steinhilber, "Structural Dynamic Investigations at the HDR, High Level Earthquake Experiment of a Piping System with Different Support Configurations," (In German), Technical Report PHDR 96–90, Sept. 1990.

21. M. G. Srinivasan, C. A. Kot and B. J. Hsieh, "Response of HDR–VKL Piping System to Seismic Test Excitations – Comparison of Analytical Predictions and Test Measurements," Trans. 10th Intl. Conf. on Structural Mechanics in Reactor Technology, Vol. K2, pp. 751–756, Anaheim, CA, 14–18 Aug. 1989.

22. J. D. Wörner, D. Schrammel and G. König, "Time–History Estimation by Using the Ultimate Load Method," Trans. 11th Intl. Conf. on Structural Mechanics in Reactor Technology, Vol. K2, paper K32/7, pp. 469–473, Tokyo, Japan, 18–23 Aug. 1991.

23. M. G. Srinivasan, C. A. Kot and M. Mojtahed, "Analytical Simulation of Nonlinear Response to Seismic Test Excitations of HDR–VKL Piping System," Trans. 11th Intl. Conf. on Structural Mechanics in Reactor Technology, Vol. K2, paper K32/6, pp. 463–468, Tokyo, Japan, 18–23 Aug. 1991.

24. C. A. Kot, M. G. Srinivasan and B. J. Hsieh, :Evaluation of Seismic Margins for an In–Plant Piping System," Trans. 11th Intl. Conf. on Structural Mechanics in Rector Technology, Vol. K2, paper K19/5, pp. 25–30, Tokyo, Japan, 18–23 Aug. 1991.

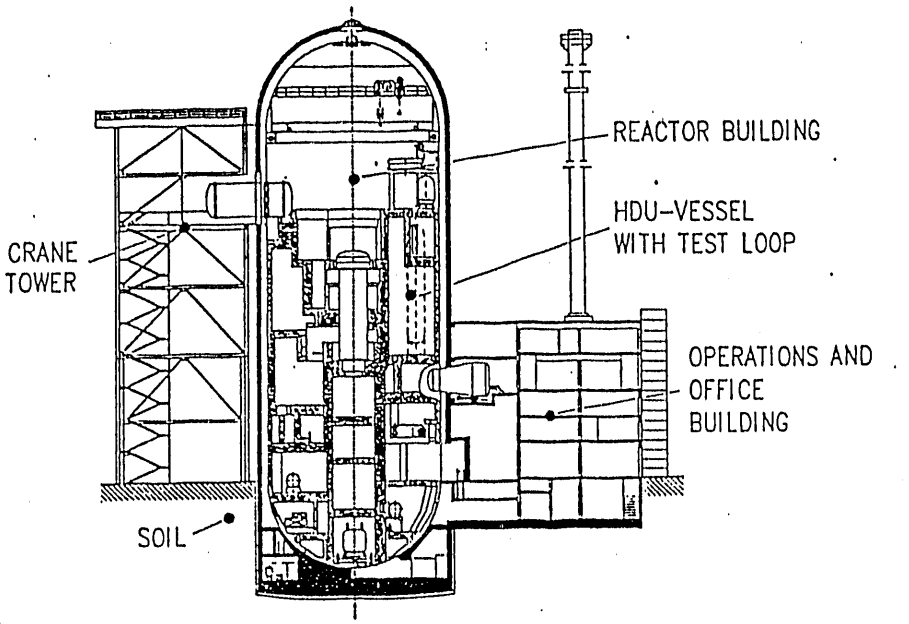

Fig. 1. HDR Reactor Building and Adjacent Structures.

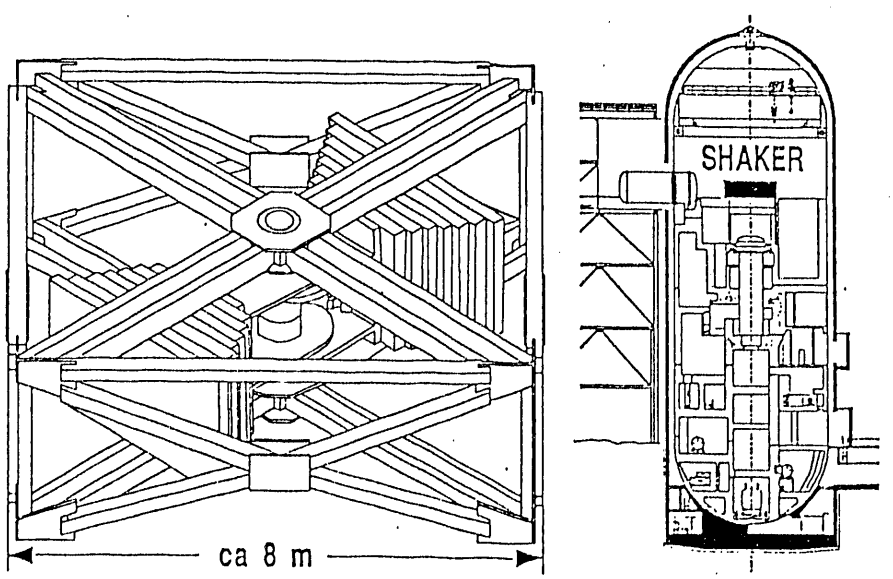

Fig. 2. Coast-Down Shaker Used in SHAG Experiements.

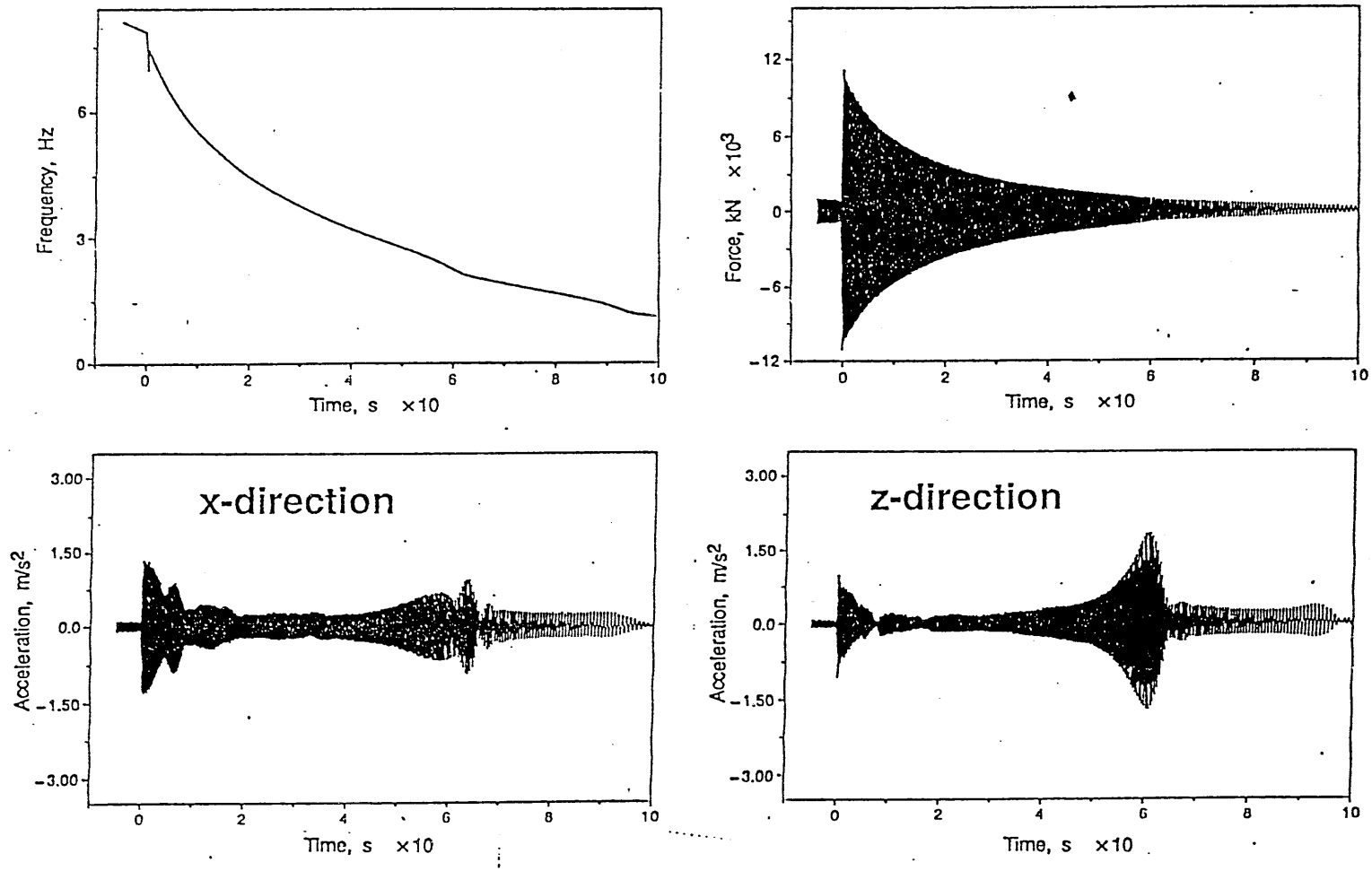

Fig. 3. SHAG Shaker Frequency, Force, and Horizontal Accelerations at Top of HDR Concrete Containment. (8-Hz Run, 4700-kgm Eccentricity.)

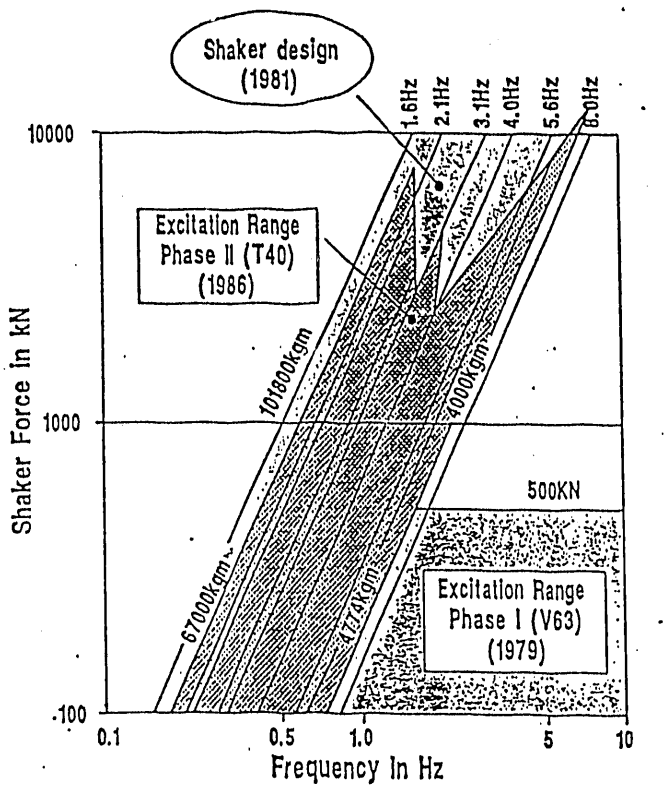

Fig. 4. Range of Excitation Load in SHAG Experiments.

		T40.13 Rocking	T40.37 Bending	Friauler E. quake	El Centro E. quake
Acceleration	(m/sec²)	1.42	1.22	1.05	0.85
Operating floor +30m	%	135	116	100	80
Displacement	(cm)	3.5	1.9	1.2	1.2
Operating floor +30m	%	292	148	100	100
Moment	(MNm)	391	335	183	173
Inner structure	%	214	183	100	95
Moment	(MNm)	400	485	101	107
Outer structure	%	396	480	100	106

Test parameter T40.13: Eccentricity 67000kgm, Starting frequency 1.6Hz
T40.37: Eccentricity 27800kgm, Starting frequency 2.1Hz

Fig. 5. Comparisons of Building Responses, SHAG Test Measurement Versus Computed for Earthquake.

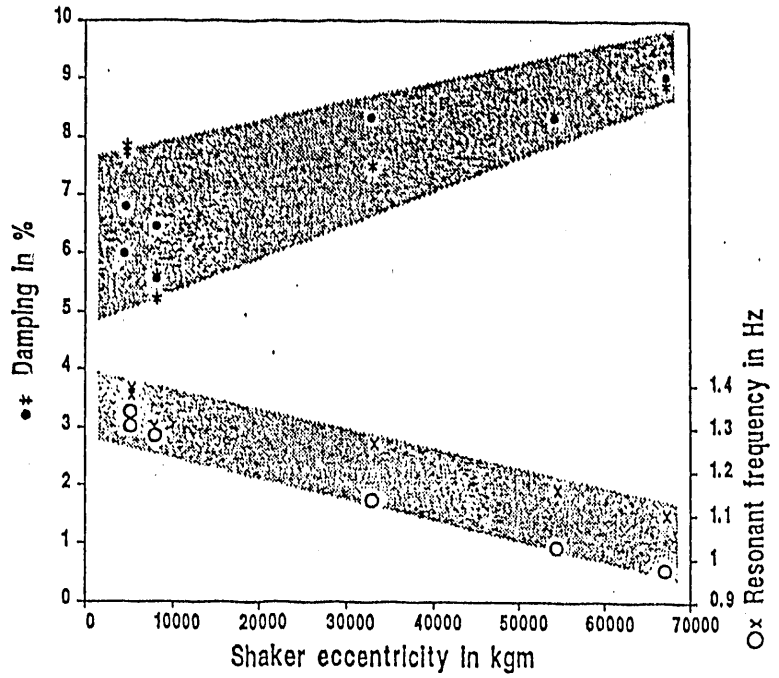

Fig. 6. Change in Rocking Mode Frequency and Damping with Shaker Load.

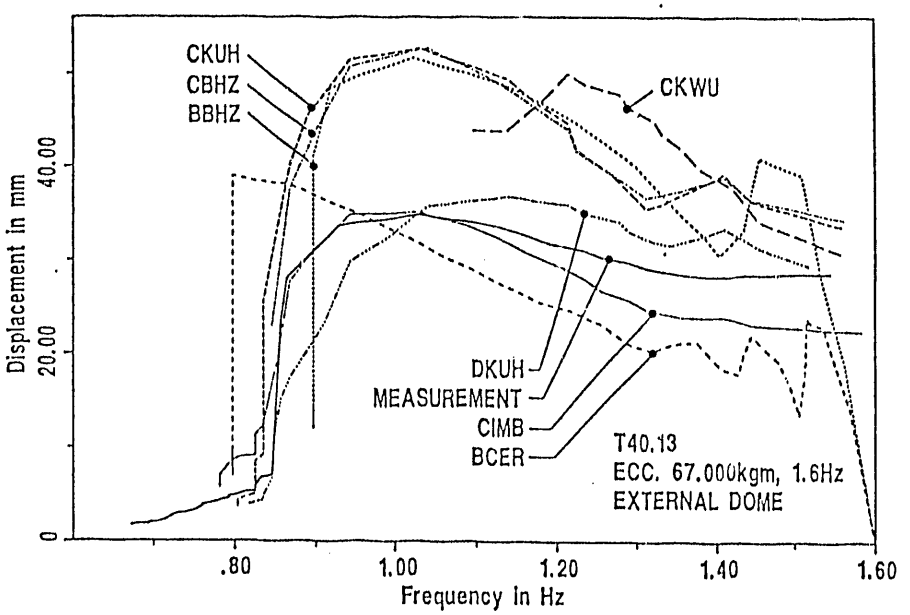

Fig. 7. Comparison of Calculated and Experimental Displacements in SHAG Test.

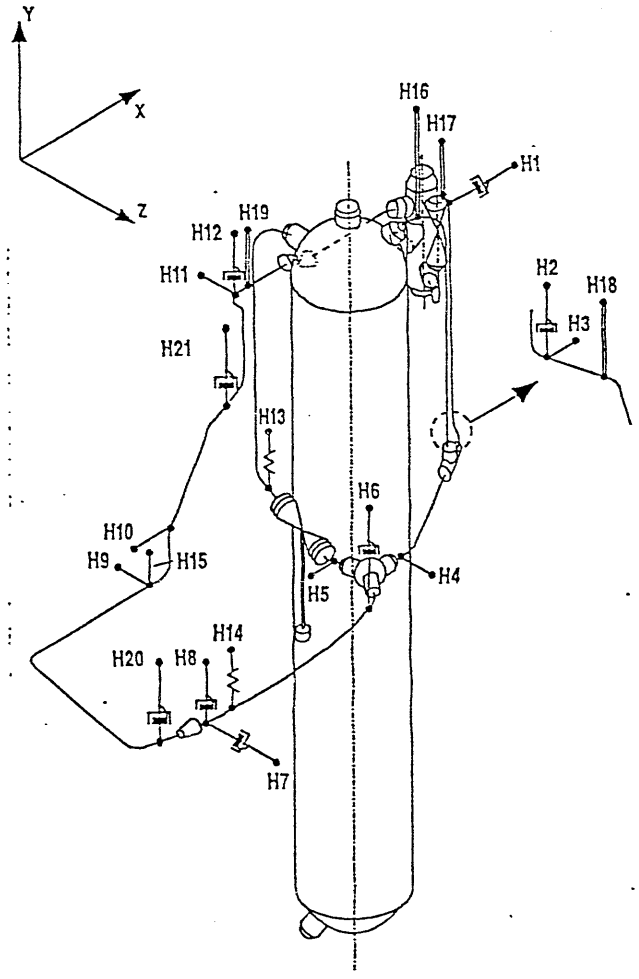

Fig. 8. Schematic of VKL Piping and Support Location in SHAG Tests.

HANGER CONFIGURATIONS

HANGER-NO.	1 HDR	2 KWU	3 NRC	4 EPRI/E.A.	5 EPRI/S.S.	7 Anco	6 Gerb
1	—	—	S.A.	E.A.	S.S.	P.D.	—
2	—	—	S.A.	—	S.S.	P.D.	—
3	—	—	STRUT				
4	STRUT						
5	STRUT						
6	—	—	S.A.	E.A.	S.S.	P.D.	—
7	—	—	S.A.	E.A.	S.S.	P.D.	—
8	—	—	S.A.	E.A.	S.S.	P.D.	—
9	—	STRUT					
10	—	STRUT					
11	—	STRUT					
12	—	—	S.A.	—	S.S.	P.D.	—
13	SPRING HANGER (NEW)						
14	SPRING HANGER (OLD)						
15	THREADED ROD						
16	CONSTANT-FORCE HANGER						
17	CONSTANT-FORCE HANGER						
18	CONSTANT-FORCE HANGER						
19	CONSTANT-FORCE HANGER						
20	—	—	—	—	—	—	P.D.
21	—	—	—	—	—	—	P.D.

S.A.: SHOCK ARRESTOR,"SNUBBER"
E.A.: ENERGY ABSORBER
S.S.: SEISMIC STOP
P.D.: PLASTIC DAMPER

Fig. 9. Hanger Configurations Used in in SHAG Tests.

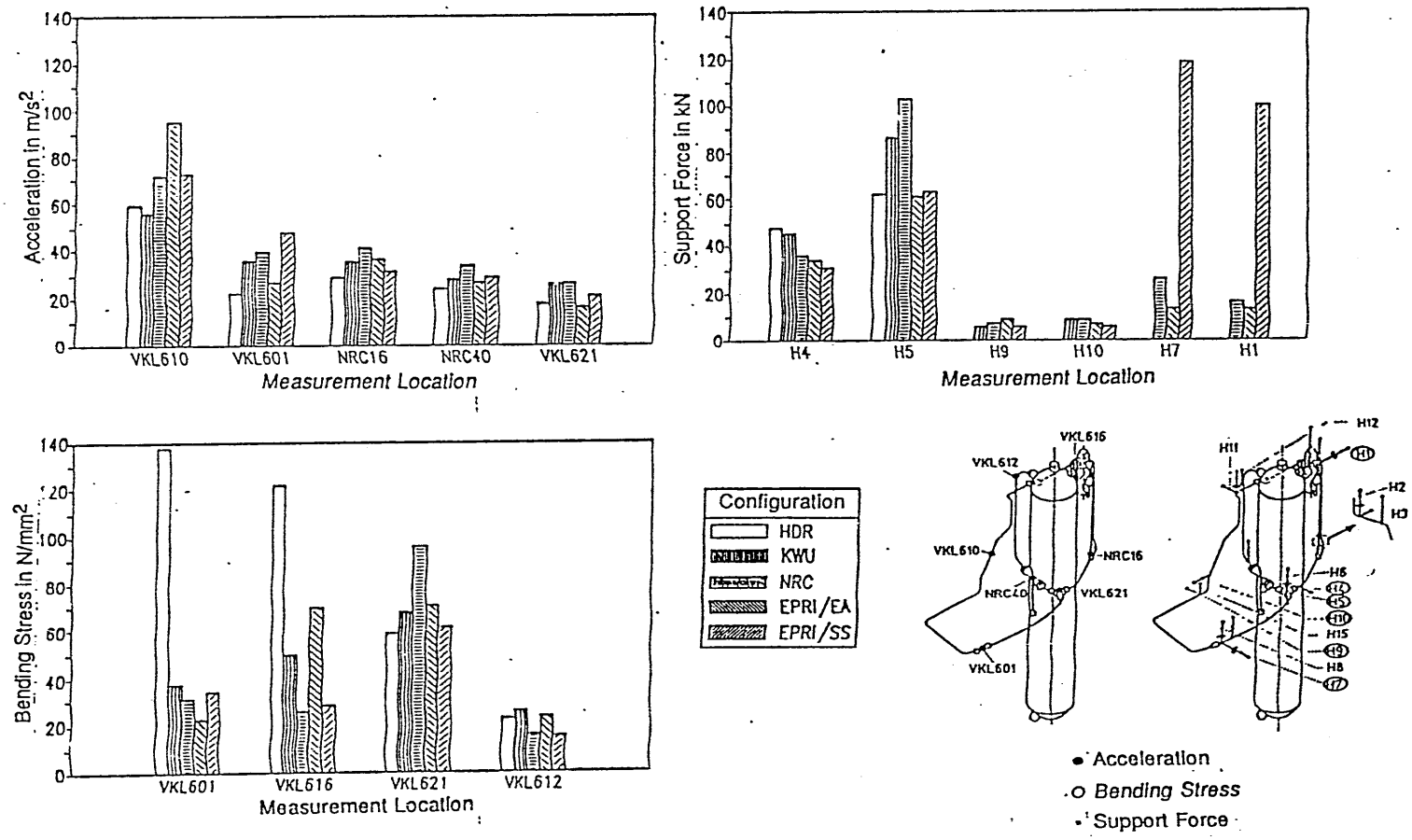

Fig. 10. Comparisons of Normalized VKL Piping Responses for the Different Support Configurations in SHAG.

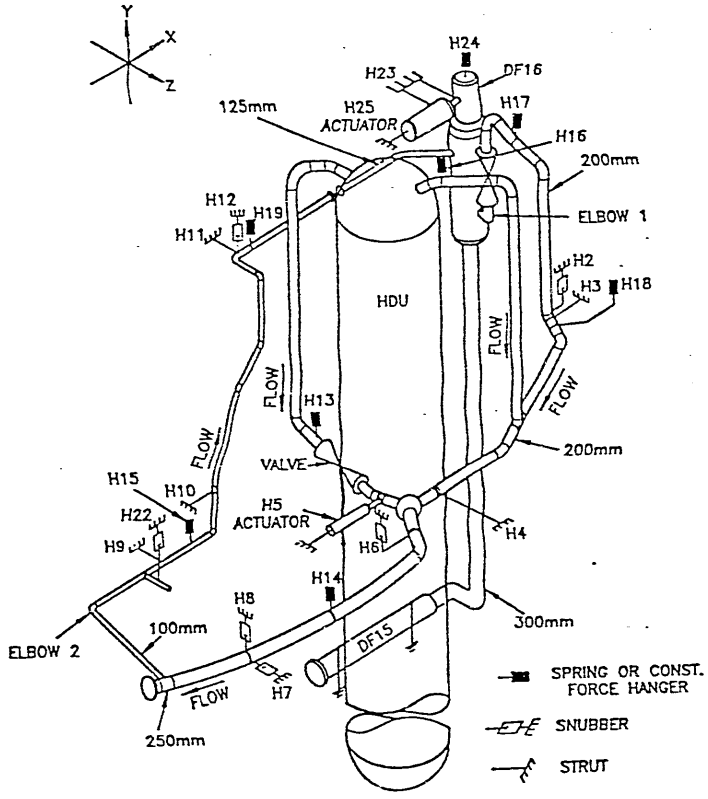

Fig. 11. VKL Piping for SHAM Experiments NRC Support Configuration.

Hanger No.	1 HDR	2 KWU	3 NRC	4 EPRI/EA	5 EPRI/SS	6 CEGB
	DYNAMIC SUPPORT CONFIGURATIONS					
2	—	—	Snubber PSA1	—	Seismic stop	—
3	—	—	Strut Size B			—
4	Strut Size 20					
6	—	—	Snubber PSA 1/2	—	Seismic stop	—
7	—	—	Snubber A/D 150	Energy Absorber	Seismic stop	Strut RS-15
8	—	—	Snubber A/D 70	Energy Absorber	Seismic stop	Strut RS-7
9	—	Strut Size B	Strut Size A			Strut RS-7
10	—	Strut Size B	Strut Size A			—
11	—	Strut Size B	Strut Size A			—
12	—	—	Snubber A/D 40	—	Seismic stop	Strut RS-15
22	—	—	Snubber PSA 1/4	Energy Absorber	Seismic stop	—
23	Two Struts 2 x Size 20					

Fig. 12. Dynamic Support Configurations for SHAM Tests.

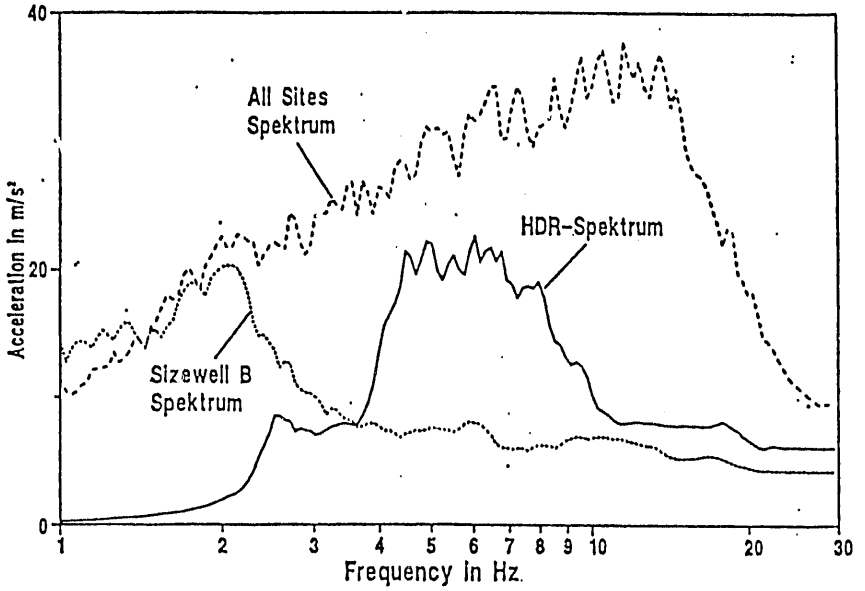

Fig. 13. Response Spectra for the 100% SSE Earthquake Excitation (4% Damping).

Typeand Location of Exitation		Hanger Configuration HDR 1	KWU 2	NRC 3	EPRI/ EA 4	EPRI/ SS 5	CEGB 6	CEGB mod. 7	NRC mod. 8
Random	DF 16	■	■	■	■	■	■		
	H-5	■	■	■	■	■	■		
Earthquake HDR - Spectrum	100 %	■	■	■ ■ ■	■	■ ■ ■	■ ■ ■		
	200 %	■	■	■		■			■
	300 %		■	■ ■	■	■			
	400 %		■		■				
	600 %		■						■
	800 %		■						■
Sizewell B Spectrum	100 %						■	■	
	300 %						■		
All Sites Spectrum	50 %						■		
	200 %						■		
Sine Burst	10 mm						■		
	20 mm						■		
	30 mm						■		
	45 mm						■		
	60 mm						■		

Fig. 14. SHAM Test Matrix.

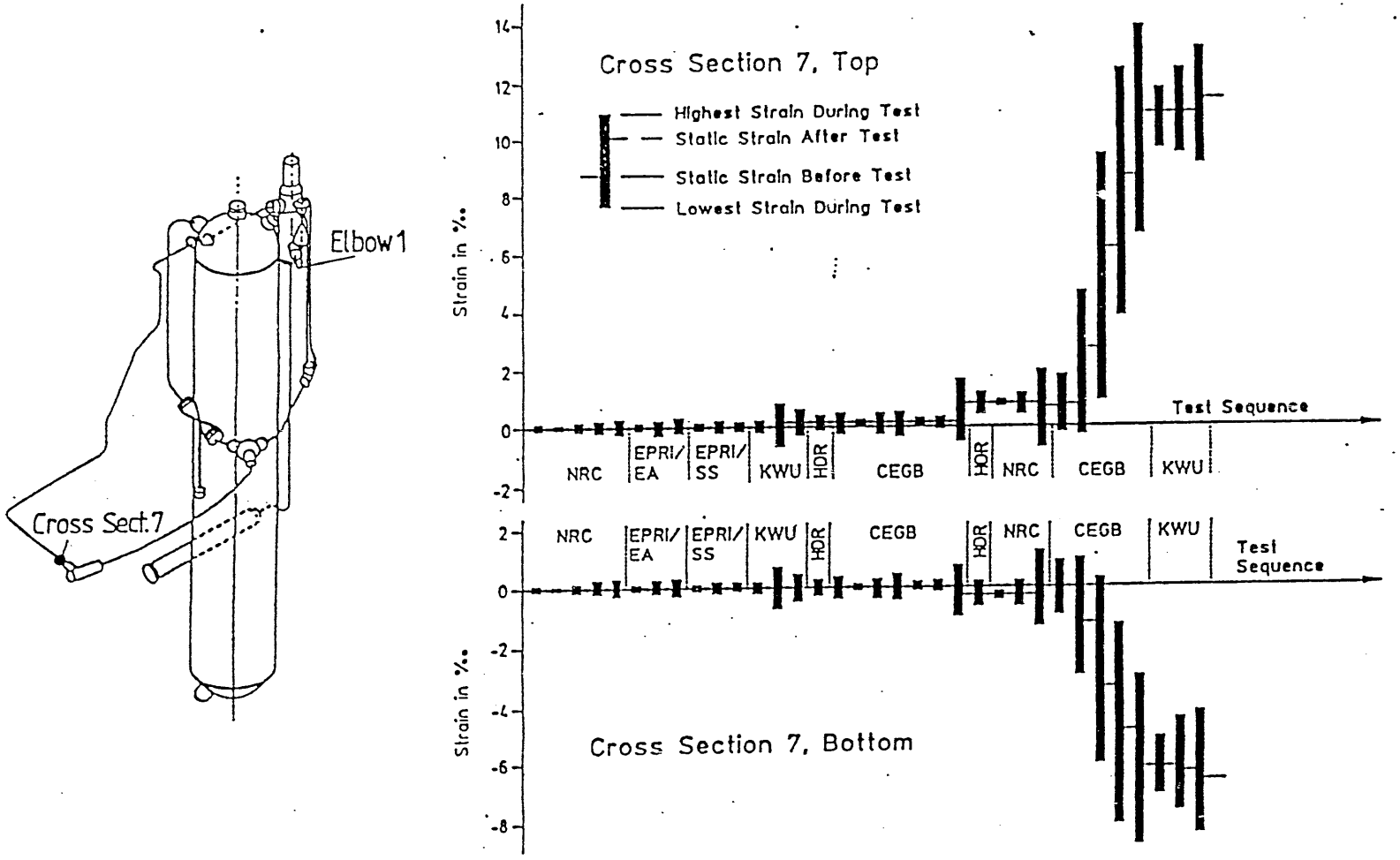

Fig. 15. Range of Strain Amplitudes and Accumulation of Permanent Strains at Cross Section 7.

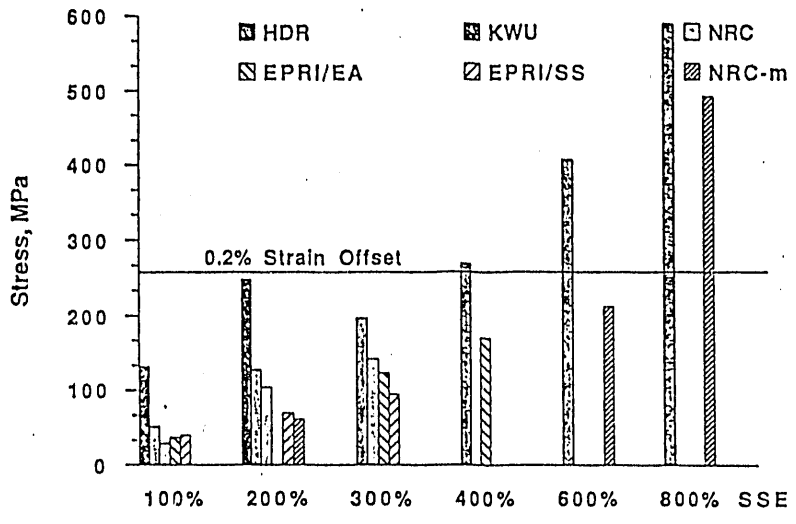

Fig. 16. Maximum Bending Stresses at Tee - 100 mm Pipe (Cross Section 7 in Fig. 15).

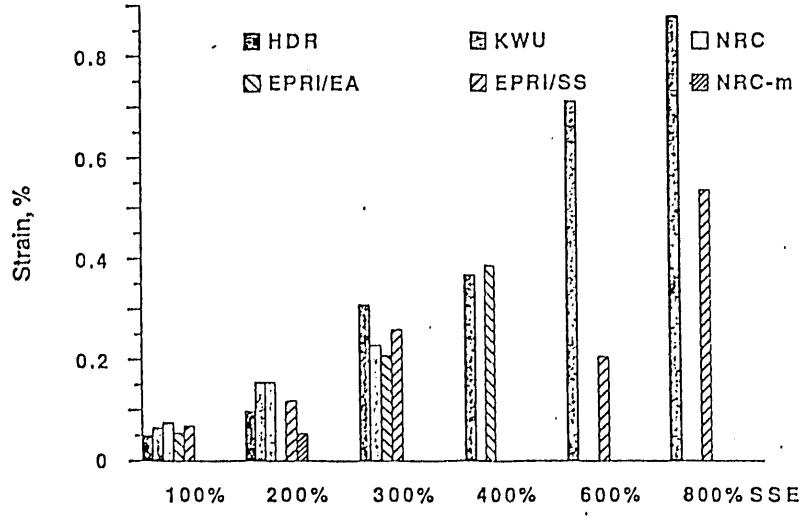

Fig. 17. Maximum Strains at Elbow 1 - 200 mm Pipe (Elbow 1 in Fig. 15).

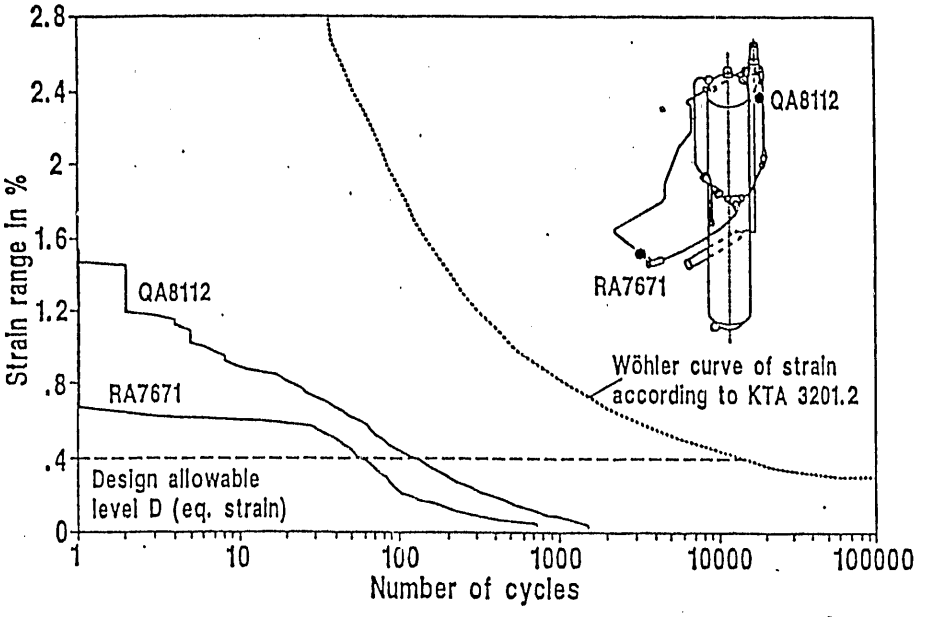

Fig. 18. Frequency Distribution of Measured Strain Amplitude Ranges Compared to Allowables: Level D Design and Fatigue Cycles.

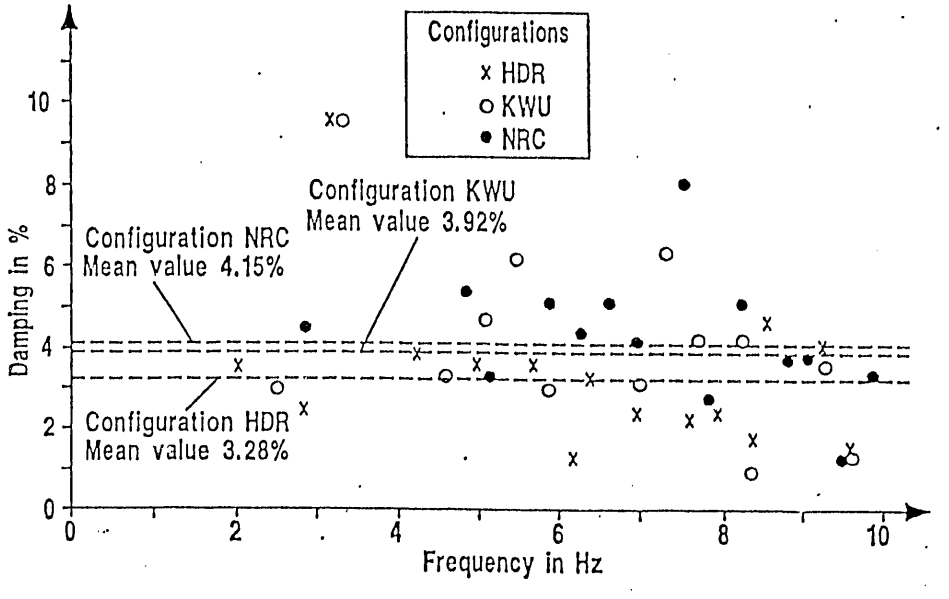

Fig. 19. VKL Piping - Modal Damping and Mean Values for Different Support Configurations (Random Tests).

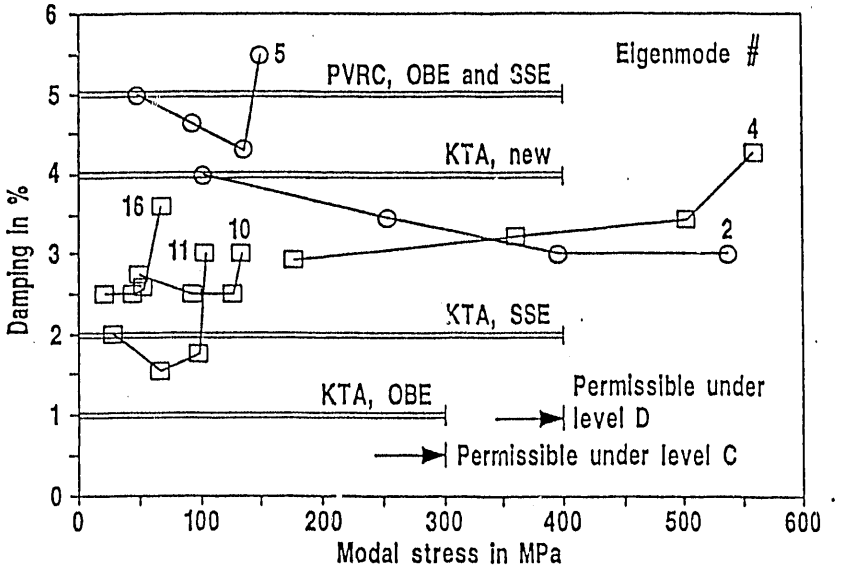

Fig. 20. Dependence of Modal Damping on Load Compared to Standard Damping Values.

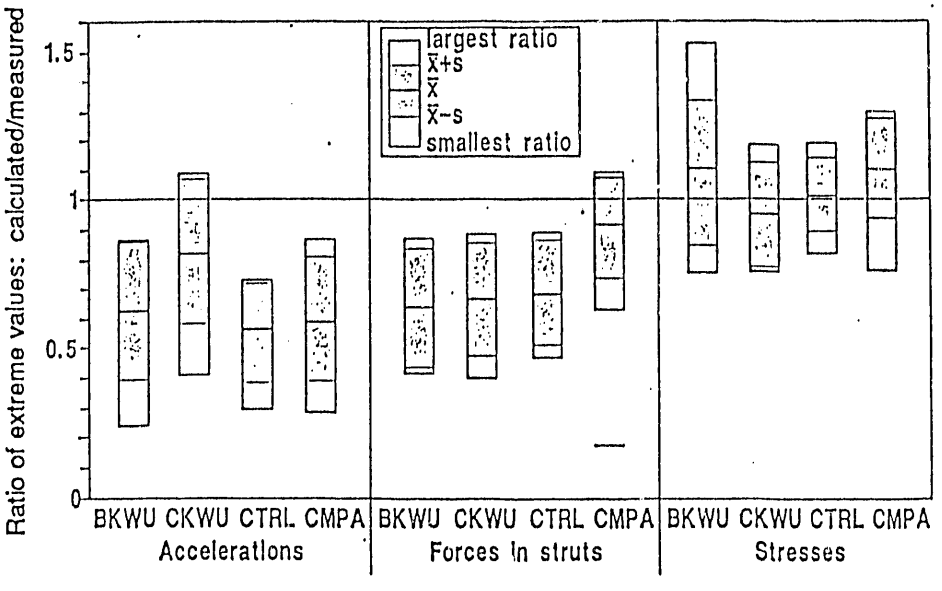

Fig. 21. Statistical Comparison of Linear German Calculations with Measurements for the 100%-SSE Test of the KWU Configuration.

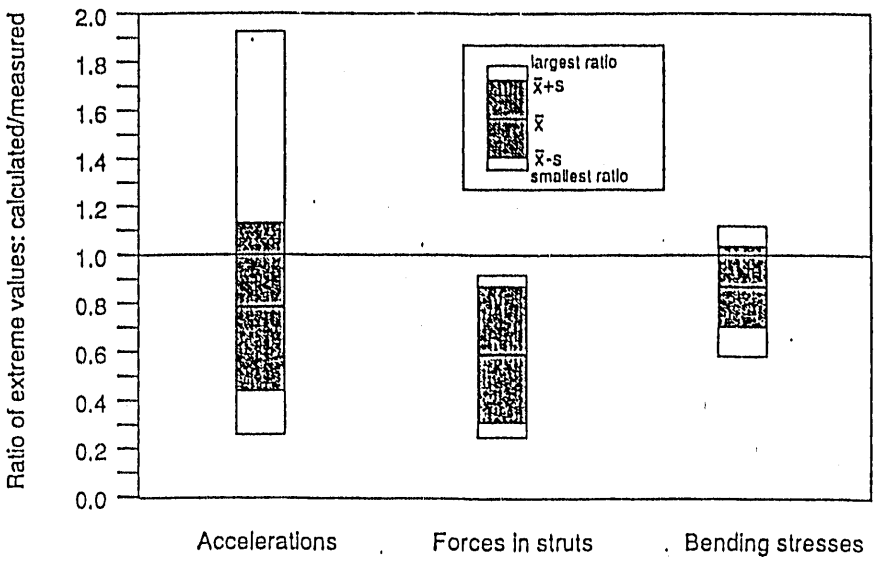

Fig. 22. Statistical Comparison of Linear (SMACS) Post-test ANL Calculations with Measurements for the 100%-SSE Test of the KWU Configuration.

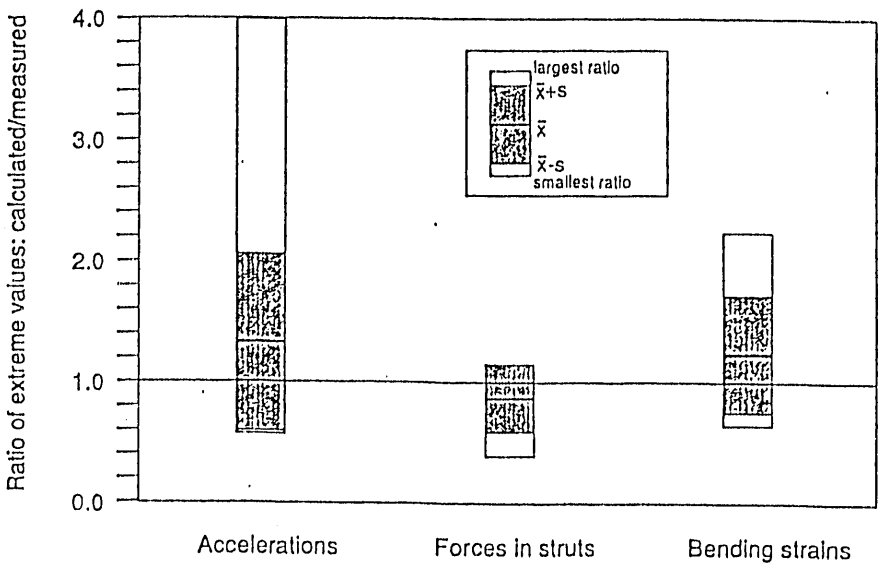

Fig. 23. Statistical Comparison of Nonlinear (NONPIPE) Post-test ANL Calculations with Measurements for the 800%-SSE Test of the KWU Configuration.

END

DATE
FILMED
3/12/92